Antioxidant Peroxiredoxin 6 protein rescues toxicity due to oxidative stress and cellular hypoxia *in vitro, and* attenuates prion-related pathology *in vivo*

Ayodeji. A. Asuni[1,4,*], **Maitea Guridi**[1], **Sandrine Sanchez**[1], and **Martin J Sadowski**[1,2,3,*]

[1]Department of Neurology, New York University School of Medicine, New York, NY 10016, USA

[2]Department of Psychiatry, New York University School of Medicine, New York, NY 10016, USA

[3]Department of Biochemistry and Molecular Pharmacology, New York University School of Medicine, New York, NY 10016, USA

[4]Centre for Biological Sciences, University of Southampton, Southampton. UK

Abstract

Protein misfolding, mitochondrial dysfunction and oxidative stress are common pathomechanisms that underlie neurodegenerative diseases. In prion disease, central to these processes is the post-translational transformation of cellular prion protein (PrP^c) to the aberrant conformationally altered isoform; PrP^{Sc}. This can trigger oxidative reactions and impair mitochondrial function by increasing levels of peroxynitrite, causing damage through formation of hydroxyl radicals or via nitration of tyrosine residues on proteins. The 6 member Peroxiredoxin (Prdx) family of redox proteins are thought to be critical protectors against oxidative stress via reduction of H_2O_2, hydroperoxides and peroxynitrite. In our *in vitro* studies cellular metabolism of SK-N-SH human neuroblastoma cells was significantly decreased in the presence of H_2O_2 (oxidative stressor) or $CoCl_2$ (cellular hypoxia), but was rescued by treatment with exogenous Prdx6, suggesting that its protective action is in part mediated through a direct action. We also show that $CoCl_2$-induced apoptosis was significantly decreased by treatment with exogenous Prdx6. We proposed a redox regulator role for Prdx6 in regulating and maintaining cellular homeostasis via its ability to control ROS levels that could otherwise accelerate the emergence of prion-related neuropathology. To confirm this, we established prion disease in mice with and without astrocyte-specific antioxidant protein Prdx6, and demonstrated that expression of Prdx6 protein in Prdx6 Tg ME7-animals reduced severity of the behavioural deficit, decreased neuropathology and increased survival time compared to Prdx6 KO ME7-animals. We conclude that antioxidant Prdx6 attenuates prion-related neuropathology, and propose that augmentation of endogenous Prdx6 protein represents an attractive adjunct therapeutic approach for neurodegenerative diseases.

---

[*]Corresponding authors. A.A. Asuni, New York University School of Medicine, 450 East 29th Street, Alexandria East River Science Park, Lab 843J, New York, NY 10016, USA. asuni@mac.com (A.A. Asuni). M. J. Sadowski, New York University School of Medicine, 450 East 29th Street, Alexandria East River Science Park, Room 830, New York, NY 10016, USA. Tel: (212) 263-0984, Fax: (646) 501-4501 sadowm01@med.nyu.edu (M.J. Sadowski).

Keywords

Neurodegeneration; Prion; ME7; Astrocytes; Peroxiredoxin 6; Antioxidant

1. Introduction

Alzheimer's disease (AD), prion disease, and Parkinson's disease (PD) are chronic protein misfolding degenerative diseases characterised by an increase in the β-sheet content and brain accumulation of misfolded amyloid-β (Aβ), prion (scrapie) protein (PrP^{Sc}), and α-synuclein respectively. This common theme in the pathogenesis of these disorders indicates that analogous degenerative processes are likely at play, and similar therapeutic strategies may be effective in these diseases. Early stages of these pathologies are characterized by localized loss of neuronal processes and synapses in the absence of overt neuron loss. The precise mechanisms of this selective synaptic degeneration is likely multifactorial (Kadish et al., 2009), involving inflammatory processes (Centonze et al., 2009), and increase in reactive oxygen species (ROS) (Mast et al., 2008) induced by physiological and/or environmental stress, allied with deficiency in bioenergetics (Kikuchi et al., 2011; Saxena, 2011). The evidence linking inflammation to disease pathogenesis is significant; involving activated astrocytes and microglia in the vicinity of misfolded proteins, activation of the classical and alternative complement pathways, and increased secretion of inflammatory cytokines (Perry et al., 2010; Raine, 2000) that can create additional ROS and peroxynitrite (PN) (Vana et al., 2011). Their generation is associated with the activation or deactivation of transcription factors capable of regulating cell survival, and down-regulation of antioxidant genes (Fatma et al., 2001; Hildeman et al., 1999), which in turn disrupts cellular integrity. Abnormally folded proteins implicated in degenerative diseases also demonstrably generate ROS, and H_2O_2 (Hensley et al., 1994; Huang et al., 1999; Pietri et al., 2006; Tabner et al., 2001), which drives further protein aggregation and oxidative damage to cells (Mao and Reddy, 2011). Mitochondria play a pivotal role in cell survival, but they are known to be a major source as well as a target for ROS (Trushina and McMurray, 2007). Malfunctions of mitochondrial metabolism as has been reported in prion pathogenesis (Choi et al., 2014; Siskova et al., 2010; Wang et al., 2009), contributes to reduced ATP production, impaired Ca^{2+} buffering and continued generation of ROS (Beal, 2007).

A number of endogenous antioxidants protect cells from ROS-induced damage. Of these, superoxide dismutase (SOD), catalase (CAT), glutathione, and selenium (SE)-dependent glutathione peroxidase (GSHPx) have been well studied. The peroxiredoxins (Prdxs); of which there are six isoforms (Prdxs1–6), belong to a relatively new group of thiol-specific antioxidants (Fisher, 2011), that are divided into two categories, the 1-Cys and 2-Cys Prdxs, based on the number of cysteine (Cys) residues directly involved in the reduction of peroxides. Prdxs1–4 belong to the "typical" 2-Cys subgroup and have additional conserved Cys residues in the COOH-terminal region (Rhee et al., 2005). Prdx5 is the single representative of the "atypical" 2-Cys Prdx class in mammalians (Rhee et al., 2005), and the Prdx6 isoform has only the NH2-terminal-conserved Cys and is, therefore, classified as a 1-Cys Prdx (Fisher, 2011). Prdx6 uses glutathione and ascorbate as electron donors and is the only member of the Prdx family that has the ability to remove H_2O_2 and phospholipid

hydroperoxides; therefore it is able to reduce the accumulation of phospholipid hydroperoxides in plasma membranes (Manevich et al., 2002). Astrocytes are the predominant source of brain Prdx6 (Asuni et al., 2014; Lafon-Cazal et al., 2003; Yang et al., 2005), and its expression has been documented in several cell compartments, including the cytoplasm, secretory organelles, lysosomes and mitochondria (Eismann et al., 2009; Immenschuh and Baumgart-Vogt, 2005; Peshenko et al., 1998; Wu et al., 2006). It is also present in CSF, plasma and urine (Brown et al., 2013).

Activation of antioxidant pathways is particularly important for tissue with relatively weak endogenous antioxidant defences, such as the brain. So, strict regulation of ROS is vital to maintain cellular integrity and homeostasis. Accrued evidence supports the notion that reduction of cellular expression and activity of SOD, CAT, and GSHPx contribute to mechanisms of aging and neurodegenerative diseases such as AD and tauopathies (Calabrese et al., 2001; Dumont et al., 2011; Facecchia et al., 2011; Pamplona and Costantini, 2011). Oxidative stress generated early in disease pathogenesis likely overwhelms endogenous antioxidant defences, leading to exacerbation of pathology. In accord, progressive increase in intracellular ROS is associated with increased accumulation of protease resistant PrP (Haigh et al., 2011), which strengthens the direct mechanistic and pathogenic association between heightened ROS and on-going prion disease pathogenesis (Canello et al., 2010; Guentchev et al., 2000; Pamplona et al., 2008; Vassallo and Herms, 2003; Wong et al., 2001). For this reason, up-regulation of ROS-detoxifying enzymes is thus a reasonable approach for amelioration of prion related pathology.

In this study we focused our efforts on examining whether overexpression of the astrocyte-specific antioxidant Prdx6 impacts prion-related neuropathology. We demonstrate biochemically that loss of Prdx6 protein exacerbates pathological indices of prion disease such as astrogliosis and accumulation of PK-resistant PrP[Sc]. Genetic overexpression of Prdx6 augmented cognitive behaviour and attenuated prion-related astrocytosis. In addition to antibody-based treatment approaches, which modulate and/or remove abnormally misfolded protein aggregates (Pankiewicz et al., 2010; Sadowski et al., 2009), other strategies to protect cells at the mitochondrial level by stabilizing or restoring mitochondrial and redox function or by interfering with energy metabolism warrant attention. Our study supports the potential utility of targeted Prdx6 augmentation as a novel adjunct treatment for neurodegenerative diseases (Pak et al., 2011; Tulsawani et al., 2010), and encouragingly results in the AD field also supports this notion (Kim et al., 2013).

2. Experimental Procedures

Ethics Statement: All procedures involving animals were approved by the Institutional Animal Care and Use Committee of the New York University and were performed in accordance with the U.K. Animals (Scientific Procedures) Act, 1986 and associated guidelines, the European Communities Council Directive of 24 November 1986 (86/609/ EEC) or the National Institutes of Health guide for the care and use of Laboratory animals (NIH Publications No. 80-23, revised 1978). All efforts were made to minimize animal suffering, and to reduce the number of animals used, and to utilize alternatives to in vivo techniques, if available. Animal Model: Age-matched nonTg C57BL6 mice (Control),

transgenic Prdx6 knockout (KO) animals and Prdx6 (Tg) overexpressing animals were used in this study, and details regarding the generation of the knockout and transgenic animals have been described previously (Phelan et al., 2003; Wang et al., 2003). Cryopreserved embryos of stock #005974 and stock #005092 were purchased and re-derived at Jackson Laboratory to generate the initial cohort of homozygous females and males Prdx6 KO and Prdx6 Tg used in the study. Mice were housed in a temperature- and humidity-controlled environment and had free access to food and water. 100 μl of 10% brain homogenate prepared from normal brains (NBH) or from terminally ill ME7-infected mice was injected intraperitoneal (i.p.) in cohorts of nonTg, Prdx6 KO and Prx6 Tg animals. Cohorts of n=12 were set up, and all mice were 5–7 weeks old at the start of the study. ME7-infected mice were killed in early stages of symptomatic disease (<20 weeks post-injection), when a blinded observer scored the animal positive on the parallel bar for 3 consecutive weeks and robust neuroinvasion could be determined biochemically. At conclusion, the mice were terminated by terminal anaesthesia and the dates were noted. The mice were perfused with heparinized saline solution, and the brains portioned; with half formalin-fixed for immunohistology or frozen in dry ice for biochemical analyses.

2.1 Behavioural assessment

Cognitive analysis of homozygous Prdx6 KO and Prdx6 Tg animals had not been previously reported; so for these studies we utilized the spontaneous novel object recognition (OR) test that requires little navigation, but is still able to measures deficits in short-term memory (Asuni et al., 2007). We reasoned that advanced prion disease related motor defects may not enable them to properly navigate the radial arm maze, which we have used extensively to assess the cognitive status of other models of neurodegeneration (Asuni et al., 2010a). OR testing was performed as we have previously described and as in those prior studies all objects tested were of equal inherent interest (Asuni et al., 2006). Following habituation and a trial phase normal mice remember a specific object over a delay up to 1 h and spend the majority of their time investigating the novel object during the retention trial. During retention tests, the animals were placed back into the same box, in which one of the previous familiar objects used during training was replaced by a second novel object, and allowed to explore freely for 6 min. The time spent exploring each object was recorded by an automatic tracking system (San Diego Instruments), and at the end of the training phase, the mouse was removed from the box for the duration of the retention delay (RD = 3 h). A different object pair was used for each trial for a given animal, and the order of exposure to object pairs as well as the designated sample and novel objects for each pair were counterbalanced within and across groups. The time spent exploring any one of the two objects (training session) is then compared to the novel one (retention session).

We assessed the competency of mice to cross a series of parallel bars that are 3 mm in diameter and are placed 7 mm apart (Sadowski et al., 2003; Sadowski et al., 2009). The earliest detectable clinical symptoms of CNS involvement in prion disease include impairment in the level of activity and competency when the mouse attempts to cross the parallel bars (Sadowski et al., 2003; Sadowski et al., 2009). The test is administered weekly by a researcher blinded to the study constituents and an animal is considered clinically symptomatic if it scores positive for disease for three consecutive weeks, after which the

animals are killed in accord with protocols approved by the New York University School of Medicine Institutional Animal Care and Use Committee.

2.2 Neuropathological Examination of Brain Sections

Coronal hippocampal sections were cut from formalin-fixed paraffin wax-embedded brains (10μm) or PLP fixed brains (40μm). As per our previous protocols the tissue were processed for immunohistology (Asuni et al., 2014; Asuni et al., 2010b). Briefly, selected sections were incubated in a humid chamber overnight at room temperature with specific antibodies. Negative control sections were covered with appropriate blocking serum while other sections were covered with primary antibody diluted in blocking buffer. Sections were scored for spongiosis, neuronal loss, gliosis, PrP^{Sc} deposition, and synaptophysin-signal intensity. Respectively, astrocytosis was detected using anti-glia fibrillary acidic protein (GFAP) polyclonal antiserum (DAKO; 1:2000 dilution), and synaptophysin was detected with Sy38 mAb (Abcam, 1:1000 dilution). Prdx6 staining was performed using rabbit anti-Prdx6 mAb (Novus biologicals; 1:500 dilution). PrP^{Sc} in brain tissue was detected after denaturation of fixed sections in formic acid using 6D11 mAb to PrP as described (Asuni et al., 2014; Asuni et al., 2010b). Sections of brains from all animals killed at each time point and from those succumbing to scrapie were examined by the same person, blinded to the identity of the animal and time of killing.

2.3 Semi-quantification of immunohistochemistry images

The images were visualized on an 80i Nikon fluorescent microscope and were captured using a high-sensitivity, cooled, monochrome DS-Qi1Mc camera and NIS Elements Imaging Software (Nikon Corp. Tokyo, Japan) and saved in a TIFF format with a resolution of 600 dpi. All images were captured using identical exposure limit, gain, saturation, shading and filter. DAB staining within the images was identified using ImageJ v.1.42 (National Institute of Mental Health, Bethesda, Maryland, USA; http://rsb.info.nih.gov/ij), with the Colour Deconvolution plugin to eliminate haematoxylin counterstain. Image threshold limit was lowered to a set level to remove background noise and kept constant for all images. Images were then converted to binary and the area of staining was measured with the "Analyze particles" routine (Schneider et al., 2012), and the percentage change in stained area was calculated with the nonTg C57BL6 animals serving as control.

2.4 Primary Cultures

Cortical neuronal cultures were prepared using neonatal 1 day old C57BL6, Prdx6 KO and Prdx6 Tg animals using a standard papain dissociation protocol (Worthington Biochemical Corporation, UK) and cultured in Neurobasal medium containing B27 supplement with 2 mM glutamine, 50 U/ml penicillin and 50 μg/ml streptomycin (Invitrogen, USA). Cells were plated onto poly-l-lysine coated plates and allowed to differentiate for 7 days before use. Cortical astrocyte cultures were prepared using neonatal 1 day old C57BL6, Prdx6 KO and Prdx6 Tg animals as previously described (Le Roux and Reh, 1996), with modifications (Kuszczyk et al., 2013). Briefly, cerebral cortex was dissected out, trypsinized, and cells cultured in minimal essential medium (MEM) supplemented by 20% FBS (Hyclone, USA), 2 mM glutamine, streptomycin (50 μg/ml) and penicillin (50 U/ml). After six days of growth the FBS content in MEM was decreased to 10%. Astrocytes were grown in 25 cm^2 flasks

until confluence. The purity of astrocytic cultures was >95% as assessed by GFAP immunostaining. Human neuroblastoma (SK-N-SH cell line # HTB-11) was obtained from the American Type Culture Collection (Manassas, VA) and cultured in minimal essential medium (MEM) supplemented with heat-inactivated 10% fetal bovine serum (FBS), penicillin (100 units/mL) and streptomycin (100 μg/mL). All the cultures were maintained at 37°C in 5% CO_2 and 95% air.

2.5 Biochemistry

Extracted brains were lysed in a buffer composed of (50 mM Tris-HCl, pH 7.4, 150 mM NaCl, 1 mM ethylene glycol tetraacetic acid (EGTA), 1 mM Na_3VO_4, 1 mM NaF, 2.5 mM $Na_4P_2O_7$, 1 mM β-glycerophosphate, 0.5% Triton, 0.5% sodium deoxycholate, 0.5 mM phenylmethylsulfonylfluoride (PMSF), protease inhibitor tablet (Roche, Indianapolis, IN, USA) or without PMSF for proteinase K (PK) digestion). To assess PK-resistant conformers of PrP, brain homogenates were treated with PK (1μg/μL) 1:20 dilution at 37°C for 1 h, according to previous methods (Pankiewicz et al., 2006; Perrier et al., 2004). After incubation, digestion is stopped by the addition of PMSF to 4 mM. Samples were then centrifuged at 20 000 *g* for 45 min at 4°C. Pellets were resuspended in 15 μL Tris-buffered saline and 15 μL sample buffer, boiled for 5 min and then resolved on SDS-PAGE gels as described previously (Jimenez-Huete et al., 1998). Homogenates were separated by SDS-PAGE and membranes were incubated with the desired primary antibodies overnight at 4°C. All antibodies were used at the manufacturers recommended dilutions and included anti-synaptophysin, GFAP, PSD-95 (all Abcam), Prdx6 (Novus biologicals) and anti-PrP 6D11 mAb (kind gift of Kascsak, RJ (Spinner et al., 2007)). In past studies following incubating of homogenates with or without PK in order to destroy the PrP[c], and retain proteinase K-resistant fragments (PrP[Sc]) it was demonstrated that an increase in PrP immunoreactivity in disease animals relates to an increasing deposition and accumulation of PrP[Sc] fragments. Hence increased anti-PrP mAb immunoreactivity is considered representative of increasing accumulation of PrP[Sc] (Asuni et al., 2014; Asuni et al., 2010a; Gray et al., 2009). The antigen-antibody complexes were detected using horseradish peroxidase-conjugated anti-mouse/rabbit/rat IgG (GE Healthcare Buckinghamshire, UK) and visualized using SuperSignal; Pierce Chemical (Rockford, IL). The exposure time was kept standard for all experiments at 1 min. Developed films were converted into eight-bit grayscale digital files using a Epson Perfection 4990 scanner (Epson America, Long Beach, CA, USA) and Adobe Photoshop software 7.01 (Adobe Systems, San Jose, CA, USA) and saved in a TIF format with a resolution of 600 dpi. Quantification of protein bands were performed by densitometric analysis of the films using NIH Image J software v. 1.42.

2.6 Protein purification

The pTAT-Prdx6 construct was generated by inserting the coding region of the human Prdx6 in the EcoR1/BamH1 sites of a pET-28b-TAT (V2.1) expression vector (kindly provided by Stephen Dowdy, University of California San Diego, San Diego, CA)(Becker-Hapak et al., 2001) in frame with the TAT/protein transduction domain peptide (YGRKKRRQRRR) (Vocero-Akbani et al., 1999). The Prdx6 cDNA inserted into the pTAT vector was generated by PCR amplification of the human cDNA. The oligonucleotides AGG ATC CAT GCC CGG AGG TCT GC and AGA ATT CTT AAG GCT GGG GT were used

as forward and reverse primers, respectively. pTAT-Prdx6 and pTAT plasmids were transformed into the Escherichia coli strain BL21(DE3), bacterial cultures were grown overnight, and protein expressions were induced by (isopropyl β-D-1 thiogalactopyranoside) treatment for 5–6 h followed by sonication in a buffer solution containing 300 mM NaCl, 10 mM Tris·HCl, 20 mM imidazole, and 8 M urea, pH 8.0 (binding buffer) in the presence of protease inhibitor cocktail (Roche). The His-tagged fusion proteins were purified using Ni^{2+}-nitrilotriacetic acid-agarose affinity column (Invitrogen, Carlsbad, CA) through a sequential wash with buffer containing 300 mM NaCl, 10 mM Tris·HCl, 50 mM imidazole, and 8 M urea, pH 8, followed by elution with a buffer containing 300 mM NaCl, 10 mM Tris·HCl, 200 mM imidazole, and 8 M urea, pH 8.0. The elutate was dialyzed against phosphate-buffered saline using the Slide-A-Lyser dialysis cassette. The TAT-fusion proteins were then desalted on a PD-10 column (GE Healthcare, Piscataway, NJ) into phosphate-buffered saline (PBS) for use.

2.7 Measurement of cell viability

Cell viability was determined by the MTT assay (Roche Diagnosis, Indianapolis, IN) as previously described (Sadowski et al., 2009). Briefly, SK-N-SH human neuroblastoma cells were seeded in at 10^4 cells/well in 96-well plates (100 μl total culture volume). Cells were exposed to 2.5 mM H_2O_2 or 50 μM $CoCl_2$ in the absence or presence of recombinant Prdx6-TAT protein (5ug/ml). 48 h after treatment, cell viability was determined. The absorbance of the solubilized MTT product was measured at 590 nm using the absorbance of cell-free wells for background subtraction. The proportion of apoptotic nuclei were assessed following chromatin staining with Hoechst 33258, and defined as the presence of two or more condensed bodies per nucleus counted. Prdx6 induced protection of the $CoCl_2$-induced cytotoxicity in astrocytes was also assessed using the MTT assay as detailed above.

2.8 Real-time semiquantitative RT-PCR (qRT-PCR)

Prdx6 mRNA expression was quantified by quantitative PCR (qRT-PCR), and the relative expression ratio was calculated based on the 2− CT method (Livak and Schmittgen, 2001). RNA was isolated using RNAeasy kit (Qiagen) and cDNA was synthesized from 500 ng of total RNA using an iScript cDNA synthesis kit (BioRad). qPCR was performed on a Bio-Rad iCycler detection system in triplicate using SYBR Green (BioRad) with Prdx6 and β-actin primers which were designed using Primer Express software (Applied Biosystems, Paisley, UK) and purchased from Sigma Genosys. Primers were as follows: β-actin forward: 5′CTA AGG CCA ACC GTG AAA AG 3′ and reverse: 5′ACC AGA GGC ATA CAG GGA CA 3′ and Prdx6 forward:5′TCA GAG TGG TTG ACT CTC TCC A 3′ and reverse 5′GGG AAC TAC CAT CAC GCT CT 3′. Cycling parameters: an initial single step at 95 °C for 10 min (denaturation) followed by 40 cycles of 94 °C for 30 s (denaturation), 60 °C for 45 s (annealing), and 72 °C for 30 s (elongation). A final elongation/termination step was performed at 72 °C for 10 min. Using the average cycle threshold (CT) calculated from multiple measurements. Mean relative expression of Prdx6 from three independent experiments (different experimental replicates) are reported normalized to control Actin.

2.9 Statistical analyses

All data are expressed as mean ± SEM unless otherwise stated. Individual data sets were tested for normality using the Shapiro-Wilk and D'Agostino & Pearson omnibus normality test. Student's t tests were applied to all data sets with two tails (two samples; unequal variance), and Mann Whitney U tests (Wilcoxon rank sum tests) were performed where data was not normally distributed. Overall, significance of differences between NBH and ME7 animals across the different strains was determined by one-way ANOVA followed by the post hoc test. Values of p<0.05 were considered to be statistically significant. Densitometric data in each bar represents means ± SEM, and One-way ANOVA -test was applied to biochemical data with a direct comparison between the nonTg and other strains. For behavioural measures, two-way ANOVA for repeated measures was used with time as the within-subject factors and NBH or ME7 infection treatment as the between-subject factors, followed by Bonferroni's post hoc tests. Two-way ANOVA was used to compare strain differences in ME7-animals. At conclusion, the termination dates of the mice were plotted on a Kaplan-Meier survival curve to demonstrate what effect the presence or absence of Prdx6 has on the different groups. Survival analysis by log-rank (Mantel-Cox) test gave a p<0.001 for ME7 Prdx6 Tg compared to ME7 Prdx6 KO animals. The median survival for ME7 Prdx6 KO animals was 185 dpi, and 195 dpi for ME7 Prdx6 Tg, compared to either NBH Prdx6 KO or NBH Prdx6 animals that did not show any mortality at these time points. Overall this represents a prolongation of the asymptomatic incubation of 10% compared to controls, respectively. None of the control animals showed signs of cerebellar ataxia through 216 days, which represented 2 weeks of continuous monitoring. All statistical analyses were made using Graph Pad Prism 6.0 (Graph Pad Software Inc., San Diego, CA, USA).

3. Results

3.1 Exogenous TAT-Prdx6 attenuates ER and oxidative stress

ER and oxidative stress are coupled to disruption of protein folding (Malhotra and Kaufman, 2011), and genetic or chemical intervention to reduce ROS species improves protein folding and cell survival and may provide an avenue to treat and/or prevent diseases of protein misfolding (Fatma et al., 2008; Malhotra et al., 2008). We examined whether exogenous Prdx6 would rescues chemically induced oxidative stress (H_2O_2) or cellular hypoxia ($CoCl_2$) in SK-N-SH human neuroblastoma cells. The capacity of the cells to reduce MTT was used as a measure of cell viability, and the results are presented as the percentage of the absorbance determined for control conditions (DMSO only) and represent the means ± SEM of duplicate experiments. As shown in (Figure 1), cell viability decreased significantly following 2.5mM H_2O_2 evoked oxidative stress, with only 45% of the cells surviving 48 h of cultivation, while over 60% survived in the presence of exogenous 5ug/ml TAT-Prdx6 (Figure 1A, *p<0.0001*). Similarly, the viability of the cells was decreased significantly to about 40% in the presence of 50uM $CoCl_2$ after 48 h (Figure 1A), and there was a rescue to about 65% in the presence of 5ug/ml exogenous TAT-Prdx6 (Figure 1A, *p<0.0001*). This is consistent with past reports showing the ability of TAT-Prdx6 to rescue cytotoxicity (Kubo et al., 2009; Wang et al., 2006). The dose used in this study was chosen based on prior published reports where cytotoxic rescue was also shown with TAT-Prdx6 (Fatma et al.,

2008; Fatma et al., 2009). They also demonstrate transduction of TAT-Prdx6 into cells (Kubo et al., 2008).

We observed that cellular damage induced by $CoCl_2$ in wild-type primary cortical neuron cells was attenuated by treatment with exogenous TAT-Prdx6 (Figure 1B, left panel), and by semi-quantitative analysis using Hoechst staining we show that $CoCl_2$-induced apoptosis was significantly decreased by treatment with 5ug/ml TAT-Prdx6 (Figure 1B, right panel). The decreases in percentages of apoptotic cells were from 40.67% in $CoCl_2$-treated cells to 19.83% in TAT-Prdx6-treated cells (*p<0.0001*) (Figure 1C). We extracted primary astrocytes from nonTg, Prdx6 KO and Prdx6 Tg animals (Figure 1D, 1E and 1F), and demonstrated a concentration dependent increase in $CoCl_2$ toxicity in all the strains. However, there were clear differences in how the cultures behaved. For example, following treatment with 1 mM $CoCl_2$, the deleterious metabolic activity was more marked in Prdx6 KO astrocytes (Figure 1D) which showed a 28.77% decrease in viability whereas both nonTg and Prdx6 Tg astrocytes (Figure 1E and 1F) only showed a 16.78% and 14.98% decrease in viability, respectively, consistent with a protective role for Prdx6 expression. These data supports the notion that overexpression of Prdx6 could attenuate neurodegeneration. So working on the hypothesis that a feasible mechanism for modulating cellular stress may be to up-regulate endogenous ROS-detoxifying enzymes, we set out to explore whether transgenic overexpressing of antioxidant Prdx6 in mice was sufficient to attenuate neurodegeneration initiated by accumulation of misfolded PrP[Sc] in prion disease.

3.2 Characterization of Prdx6 animals

Initial studies were carried out to confirm and characterize the expression of Prdx6 in the brains of homozygous Prdx6 Tg animals and its absence in homozygous Prdx6 KO animals. Biochemical data revealed that naïve unstimulated primary neurons did not express detectable Prdx6, whereas in primary astrocytes and brain homogenates from Prdx6 Tg and nonTg animals there was expression of Prdx6 compared to Prdx6 KO animals (Figure 2A). There was a significant 15.22-fold increase in Prdx6 protein levels in astrocytes from nonTg compared Prdx6 Tg animals (*p<0.001*) (data not shown), and we observed an equally marked 4.48-fold increase in Prdx6 protein expression in whole brain homogenates from nonTg compared Prdx6 Tg animals (*p<0.001*) (data not shown). This is consistent with prior described astrocytic expression of Prdx6, and supported by Prdx6 mRNA analysis showing that the brains of Prdx6 Tg mice exhibit an approximately 15-fold increase in Prdx6 mRNA compared with the nonTg animals (Figure 2B, *p<0.001*) while there was no expression of Prdx6 mRNA in Prdx6 KO animals compared to nonTg animals (Figure 2B, *p<0.001*). Prdx6 has previously been characterized in C57BL6 mouse by *in situ* hybridization, and was demonstrated to be expressed in discrete regions of the brain including the cortex and hippocampus (Figure 2C). We examined the brain expression pattern of Prdx6 in nonTg, Prdx6 KO and Prdx6 Tg animals by immunohistology. As expected, there was no expression of Prdx6 in Prdx6 KO animals (Figure 2D, *middle panel*), and there was some staining in nonTg animals (*left side panel*), in contrast to the robust staining we observed in Prdx6 Tg animals (Figure 2D, *right side panel*). Prdx6 immunoreactivity (IR) in Prdx6 Tg animals is distributed around the brain in a mosaic pattern and appears to decorate astrocyte-like structures, consistent with astrocytes being the predominant source of brain Prdx6. The

Prdx6 IR in some cells decorates the neuropil reminiscent of dye-filled astrocytes with fine processes.

3.3 Behavioural changes in Prdx6 KO and Prdx6 Tg animals

Prior to initiating prion pathology Prdx6 KO and Prdx6 Tg animals were weighed to determine if there were any atypical transgene-associated differences, and we did not observe any differences as Prdx6 Tg animals weighed 22.16 ± 0.28g while Prdx6 KO animals weighed 21.88 ± 0.31g respectively. Cohorts of animals were inoculated with normal brain homogenate (NBH), and pathological ME7 strain of prion, and were monitored biweekly and their weights measured, and we saw no differences in the course of this study (Figure 3A). Based on our prior experience we anticipated these animals would begin to show obvious pathology after 150 days post inoculation (dpi), and monitored them more closely once this time had elapsed. Using our established protocols mice were subjected to weekly behavioural testing on traverse parallel bars to monitor clinical signs of prion infection using a test of motor co-ordination for three consecutive weeks by an observer blinded to the experimental status of the animals (data not shown). Animals were sacrificed after 3 weeks of positive scoring. Differences in Kaplan-Meier survival curves of nonTg NBH, nonTg ME7, Prdx6 KO NBH, Prdx6 KO ME7, Prdx6 Tg NBH and Prdx6 Tg ME7 were analyzed by the Log-rank test (Figure 3B). Kaplan-Meier survival curves revealed that loss of Prdx6 in Prdx6 KO ME7-animals significantly worsened survival compared to Prdx6 expression in Prdx6 Tg ME7-animals which extended median survival by 10 days (Figure 3B). Prdx6 KO ME7 compared to Prdx6 Tg ME7 $p<0.0004$ (Mantel-cox) (Figure 3B), but nonTg ME7 were not significantly different from Prdx6 Tg ME7 ($p=0.0918$). These animals were also subjected to a novel object recognition task, which revealed that both nonTg ME7-animals and nonTg NBH-animals could discriminate novel from old objects (Figure 3C, $p=0.011$ and $p=0.026$, respectively), but there was no difference in their ability to discriminate novel objects ($p=0.714$). Prdx6 KO NBH-animal could significantly discriminate novel from old objects (Figure 3D, $p=0.0013$), whereas Prdx6 KO ME7-animals could not ($p=0.402$), and Prdx6 KO NBH-animal spent significantly more time with the novel objects than Prdx6 KO ME7-animals ($p=0.0008$). Conversely both Prdx6 Tg ME7-animals and Prdx6 Tg NBH-animals could discriminate novel from old objects (Figure 3E, $p=0.0001$ and $p=0.0042$, respectively) but Prdx6 Tg NBH-animals spent significantly more time with the novel object than Prdx6 ME7-animals ($p<0.0001$). Prdx6 KO ME7-animals spent the least time with the novel objects, in contrast to nonTg ME7- and Prdx6 Tg ME7-animals (Figure 3F, 37.8% compared to 55.7%, and 55.8% for nonTg and Prdx6 Tg respectively). Furthermore, all cohorts of NBH-animals were able to discriminate novel objects, but Prdx6 Tg NBH-animals showed the most preference for the novel objects (Figure 3G, 80.56% compared to 62%, and 59% for non Tg and Prdx6 KO, respectively).

3.4 Altered prion-related pathology in Prdx6 KO and Prdx6 Tg animals

To determine whether the altered behaviour effect observed in Prdx6 Tg ME7-animals translated into pronounced changes in biochemical correlates of prion pathology, animals were sacrificed in early stages of symptomatic disease (after 3 weeks of positive scoring) when there was significant accumulation of misfolded PrP^{Sc} and no overt neuronal loss. We measured the extent of pathology by quantitative biochemical estimates of protein changes

in brain extracts from control, and ME7-animals. We observed a significant increase in PrP (PrP^c/PrP^{Sc}) immunoreactivity (IR) in nonTg-, Prdx6 KO- and Prdx6 Tg-ME7 compared to NBH-animals at the same time point (Figure 4A, *panel i*; Figure 4B, *graph i*). Concomitantly there was significantly less accumulated PK resistant PrP^{Sc} in Prdx6 Tg ME7-animals compared to Prdx6 KO-ME7-animals (Figure 4A, *panel ii*; Figure 4B, *graph ii; p<0.05*), but there was no significant difference in the PrP^{Sc} IR in nonTg-ME7 compared to Prdx6 KO-ME7. NonTg NBH-animals expressed Prdx6 protein, but there was additional induction in nonTg ME7-animals (Figure 4A, *panel iii*; Figure 4B, *graph iii; p<0.05*). As anticipated there was no Prdx6 expression in the cohorts of Prdx6 KO animals used (Figure 4A and Figure 4B, *graph iii*). There was robust expression of Prdx6 protein in both Prdx6 Tg NBH- and Prdx6 Tg ME7-animals but the levels were not significantly different (Figure 4A and Figure 4B, *panel iii*), but the levels were significantly different from expression in nonTg animals (*p<0.001,* respectively). As a marker of prion-related neuropathology, GFAP IR was significantly increased in all ME7-animals, but there was significantly less in Prdx6 Tg ME7-animals compared Prdx6 KO ME7-animals (Figure 4A, *panel iv*; Figure 4B, *graph iv; p<0.001*), as a muted ME7 pathology was generated in Prdx6 Tg animals. Synaptophysin immunoreactivity was not markedly decreased in either cohort of animals (Figure 4A, *panel v*; Figure 4B, *graph v)*, and there was no change in the expression of (post synaptic density protein) PSD-95 in nonTg, Prdx6 KO and Prdx6 Tg ME7 compared to NBH-animals (*not shown*).

We examined prion-related gliosis and synaptopathy by DAB immunostaining and semi-quantitatively measured the difference in DAB intensity in the hippocampus of both the Prdx6 Tg and Prdx6 KO ME7-animals and expressed this as a percent immunoreactivity relative to similarly stained sections from nonTg ME7-animals. We show that there was markedly increased GFAP IR in the hippocampus of nonTg ME7- and Prdx6 KO ME7-animals, which was significantly different from that in Prdx6 Tg ME7-animals (Figure 5A–D, *p<0.05 respectively*). In nonTg ME7- and Prdx6 KO ME7-animals hippocampal synaptophysin staining was significantly decreased compared to Prdx6 Tg ME7-animals, (Figure 5E–H, *p<0.05* and *p<0.001* respectively), but more indicative of this is the loss of demarcated synaptic layers and increasing disorganisation of synaptic architecture (depicted in Figure 5I) in nonTg ME7- and Prdx6 KO ME7-animals compared to Prdx6 Tg ME7-animals.

4 Discussion

4.1 Prdx6 is cytoprotective against chemically induced oxidative stress and hypoxia

To demonstrate Prdx6 mediated antioxidant capacity, we examined whether exogenous Prdx6 would rescue chemically evoked oxidative stress and activation of mitochondrial-apoptotic pathway (H_2O_2 and $CoCl_2$) in SK-N-SH human neuroblastoma cells. We showed that cell viability decreased significantly in the presence of 2.5 mM H_2O_2, with only 45% of the cells surviving 48 h of cultivation, while over 60% survived in the presence of exogenous TAT-Prdx6. We also observed that the viability of SK-N-SH human neuroblastoma cells was significantly decreased by about 40% in the presence of 50uM $CoCl_2$ after 48 h, and once again it was rescued with an application of exogenous TAT-

Prdx6. This is consistent with past results showing the ability of Prdx6 to rescue cytotoxicity (Kubo et al., 2009; Tulsawani et al., 2010; Wang et al., 2006). Semi-quantitative analysis using Hoechst staining showed that $CoCl_2$-induced apoptosis was significantly decreased by treatment with TAT-Prdx6. The decreases in percentages of apoptotic cells were from 41% in $CoCl_2$-treated cells to approximately 20% in Prdx6-treated cells ($p<0.0001$). The altered neuronal homeostasis and synaptic integrity represented by dendritic dystrophy we observed in $CoCl_2$ cortical neurons is in contrast to the intact complex dendritic network with smooth and long dendritic arborization visible in 5ug/ml TAT-Prdx6 augmented cells. So given the cytoprotective effect of Prdx6 on H_2O_2 a n d $CoCl_2$ treated neuroblastoma cells we postulated that Prdx6 could metabolize peroxides generated as a consequence of prion induced oxidative stress, thus protecting cells as prion-related neuropathology ensues.

4.2 Redox dysfunction in chronic degenerative disorders

Strict regulation of ROS is vital to maintain cellular integrity and homeostasis, and activation of antioxidant pathways are particularly important for the brain with relatively weak endogenous antioxidant defences. So unsurprisingly, reduction of cellular expression and activity of antioxidant proteins are known corollary of aging and neurodegenerative diseases (Calabrese et al., 2001; Dumont et al., 2011; Pamplona and Costantini, 2011). This oxidative stress is be the consequence of an increased production of reactive species, a decrease in the capacity of antioxidant defenses to remove them, or both. In prion disease, PrP[Sc] may trigger oxidative reactions by various means including by increasing levels of peroxynitrite, which can then cause damage through the formation of hydroxyl radicals or via nitration of tyrosine residues on proteins (Guentchev et al., 2000). We previously demonstrated a significant upregulation of Clusterin, GFAP, EAAT-2 and Prdx6 in ME7- compared to NBH-animals (Asuni et al., 2014). Primarily this increase in astrocyte- expressed proteins reinforced the notion that astrocytes are significant contributors to disease mechanisms (Gray et al., 2006; Lazarini et al., 1994), but we also considered that increased expression of antioxidant Prdx6 represents a physiological response initiated to modulate the redox dysfunction and associated neurodegeneration initiated by misfolded PrP[Sc]. This lead us to explore whether transgenic overexpressing of antioxidant Prdx6 in mice was sufficient to attenuate neurodegeneration initiated by accumulation of misfolded PrP[Sc] in prion disease.

4.3 Prdx6 attenuates prion-related pathology in vivo

We showed that Prdx6 expression was predominant in astrocytes of nonTg, and Prdx6 Tg animals, with no expression in Prdx6 KO animals. The animals were then inoculated with either NBH or pathological ME7 strain of prion. At the first evidence that these animals scored positive for scrapie for 3 weeks, we subjected the animals to a mild cognitive test. Both nonTg and Prdx6 Tg NBH- and ME7-aniamls could clearly discriminate novel from old objects, but compared to Prdx6 KO NBH-animals, Prdx6 KO ME7-animals showed significant reduction in their ability to discriminate novel from old objects, which we interpret to mean that prion-induced neuropathology more adversely impacted mild cognition in these animals. Interestingly Prdx6 Tg NBH-animals also spent significantly more time with the novel object than nonTg NBH-animals which suggests added Prdx6 augmentation of their ability to discriminate novel objects. Remarkably, based on time of

sacrifice post-disease onset Kaplan-Meier survival curves were generated which showed a significant 10 days prolongation of asymptomatic incubation period of prion infection in Prdx6 Tg ME7- compared to Prdx6 KO ME7-animals ($p<0.05$). There was also a difference compared the nonTg ME7-aniamls which was not significant.

Our biochemical analyses reveal significant increase in PrP load in ME7- compared to NBH-animals, but there was demonstrably more PrP load in Prdx6 KO ME7- compared to Prdx6 Tg ME7-animals. Proteinase K digestion liberated pathological PrP[Sc] in the brains of these animals, and there was a significant decrease in pathological PrP[Sc] in Prdx6 Tg ME7- compared to Prdx6 KO ME7-animals. Our biochemical data also showed significantly less astrocytosis in Prdx6 Tg ME7- compared to Prdx6 KO ME7- and nonTg ME7-animals; but synaptophysin immunoreactivity was not markedly different when quantified by western blotting. This is likely because whole brain homogenates were utilised for this measure. Consistent with the remaining biochemical data, our histological analysis revealed less astrocytosis in Prdx6 Tg ME7- compared to Prdx6 KO ME7- and nonTg ME7-animals; and shows a pronounced loss of synaptophysin immunoreactivity, and synaptic demarcation. Our results demonstrate that lack of Prdx6 negatively impacts prion-related neuropathology and associated behaviour, and confirmed that the presence of antioxidant Prdx6 attenuates prion-related neuropathology. Gene expression of Peroxiredoxin 1–5, glutaredoxin 1–4, catalases, superoxide dismutases 1–3, thioredoxin 1–2, and glutathione peroxidases 1–2 antioxidant is not different between Prdx6 KO and control animals (Wang et al., 2003), suggesting that the Prdx6 antioxidant properties in these mice was independent of other antioxidant enzymes.

NonTg NBH-animals expressed Prdx6 protein, but there was additional induction in nonTg ME7-animals, suggestive of its protective induction in response to the accumulation of PrP[Sc]. In accord nonTg ME7- compared to nonTg NBH-animals, both Prdx-6 and PrP mRNA appear unchanged (Asuni et al., 2014), which would support that the increased expression of these proteins is due solely to post-translational modification, mediated by the increasing accumulation of misfolded protein. We would hypothesize that as a result of increased Prdx6 expression, mitochondria from Prdx6 Tg mice may produce significantly reduced amount of H_2O_2, and cells from Prdx6 Tg mice could have increased resistance to stress-induced cell death and apoptosis. A balance between the pro-oxidant and anti-oxidant levels exists under physiological conditions; however, other factors or disease cause an imbalance leading to increased production of stressors like ROS. Increased ROS perpetuates the degenerative cascade, by increasing production of toxic lipid peroxidation products, which further contributes to oxidative stress-induced cell death. Others have documented increased levels of lipid peroxidation in prion disease (Brazier et al., 2006).

There is indeed prior precedent for astrocyte-mediated neuroprotection in neurodegenerative disease (Shao et al., 2012; Yata et al., 2011), and in this study we observed significant protective effects of exogenous TAT-Prdx6 in acute *in vitro* systems, and we show that expression of astrocyte-specific antioxidant protein Prdx6 in Prdx6 Tg ME7-animals reduced severity of the clinical abnormalities, improved neuropathology and increased survival time compared to Prdx6 KO ME7-animals. Over time prion disease mediates chronic, low-levels of oxidative stress, likely overwhelming protective responses and

altering cellular homeostasis, therefore dramatic protective effects are not evident in the Prdx6 ME7- compared to Prdx6 KO ME7- or nonTg ME7-animals.

Knockdown of Prdx6 resulted in increased sensitivity to oxidative injury (Manevich et al., 2002; Pak et al., 2002), similar to observations made in Prdx6 null animals (Wang et al., 2003). SOD1, another endogenous antioxidant has also been shown to attenuate prion-related pathology (Akhtar et al., 2013). Our rationale for pursuing Prdx6's protective effect is based on the hypothesis that at least in part, mitochondrial and ER stress, precipitated by the accumulation of specific misfolded proteins (prion or Aβ or α-synuclein) significantly contributes to disease pathogenesis (Bredesen, 2008; Hara and Snyder, 2007; Siskova et al., 2010), and a desirable therapeutic approach would be one designed to upregulate astrocytic neuroprotective capacity without inducing inflammatory cytokines. Based on these data, we propose a redox modulator role for Prdx-6 in regulating and maintaining cellular homeostasis via its ability to control the ROS levels and suppress the activation of detrimental signalling pathways. Despite abundant evidence of a significant role for oxidant in the CNS degeneration, only few oxidant protective approaches have been employed, with inconclusive results and very limited success (Adair et al., 2001; Galasko et al., 2012; Hager et al., 2007; Markesbery, 1999; Subbarao et al., 1990). We are encouraged by a recent study which shows Prdx6-mediated protection against Aβ pathology *in vitro* (Kim et al., 2013). TAT-Prdx-6 has been shown to attenuate neurotoxicity *in vitro*, and may similarly have potential to prevent degeneration *in vivo* (Kubo et al., 2008). We believe augmentation of endogenous Prdx6 protein represents an attractive adjunct therapeutic approach for neurodegenerative diseases, and these findings provide a foundation for rational development of antioxidant-based therapeutics for acute and chronic degenerative diseases.

Acknowledgments

References

Adair JC, Knoefel JE, Morgan N. Controlled trial of N-acetylcysteine for patients with probable Alzheimer's disease. Neurology. 2001; 57:1515–1517. [PubMed: 11673605]

Akhtar S, Grizenkova J, Wenborn A, Hummerich H, Fernandez de Marco M, Brandner S, Collinge J, Lloyd SE. Sod1 deficiency reduces incubation time in mouse models of prion disease. PLoS One. 2013; 8:e54454. [PubMed: 23349894]

Asuni AA, Boutajangout A, Quartermain D, Sigurdsson EM. Immunotherapy targeting pathological tau conformers in a tangle mouse model reduces brain pathology with associated functional improvements. J Neurosci. 2007; 27:9115–9129. [PubMed: 17715348]

Asuni AA, Boutajangout A, Scholtzova H, Knudsen E, Li YS, Quartermain D, Frangione B, Wisniewski T, Sigurdsson EM. Vaccination of Alzheimer's model mice with Abeta derivative in alum adjuvant reduces Abeta burden without microhemorrhages. Eur J Neurosci. 2006; 24:2530–2542. [PubMed: 17100841]

Asuni AA, Gray B, Bailey J, Skipp P, Perry VH, O'Connor V. Analysis of the Hippocampal Proteome in ME7 Prion Disease Reveals a Predominant Astrocytic Signature and Highlights the Brain-restricted Production of Clusterin in Chronic Neurodegeneration. J Biol Chem. 2014; 289:4532–4545. [PubMed: 24366862]

Asuni AA, Hilton K, Siskova Z, Lunnon K, Reynolds R, Perry VH, O'Connor V. Alpha-synuclein deficiency in the C57BL/6JOlaHsd strain does not modify disease progression in the ME7-model of prion disease. Neuroscience. 2010a; 165:662–674. [PubMed: 19879926]

Asuni AA, Perry VH, O'Connor V. Change in tau phosphorylation associated with neurodegeneration in the ME7 model of prion disease. Biochem Soc Trans. 2010b; 38:545–551. [PubMed: 20298219]

Beal MF. Mitochondria and neurodegeneration. Novartis Found Symp. 2007; 287:183–192. discussion 192–186. [PubMed: 18074639]

Becker-Hapak M, McAllister SS, Dowdy SF. TAT-mediated protein transduction into mammalian cells. Methods. 2001; 24:247–256. [PubMed: 11403574]

Brazier MW, Lewis V, Ciccotosto GD, Klug GM, Lawson VA, Cappai R, Ironside JW, Masters CL, Hill AF, White AR, Collins S. Correlative studies support lipid peroxidation is linked to PrP(res) propagation as an early primary pathogenic event in prion disease. Brain Res Bull. 2006; 68:346–354. [PubMed: 16377442]

Bredesen DE. Programmed cell death mechanisms in neurological disease. Curr Mol Med. 2008; 8:173–186. [PubMed: 18473818]

Brown KJ, Seol H, Pillai DK, Sankoorikal BJ, Formolo CA, Mac J, Edwards NJ, Rose MC, Hathout Y. The human secretome atlas initiative: Implications in health and disease conditions. Biochimica et Biophysica Acta (BBA) - Proteins and Proteomics. 2013; 1834:2454–2461. [PubMed: 23603790]

Calabrese V, Scapagnini G, Giuffrida Stella AM, Bates TE, Clark JB. Mitochondrial involvement in brain function and dysfunction: relevance to aging, neurodegenerative disorders and longevity. Neurochem Res. 2001; 26:739–764. [PubMed: 11519733]

Canello T, Frid K, Gabizon R, Lisa S, Friedler A, Moskovitz J, Gasset M, Gabizon R. Oxidation of Helix-3 methionines precedes the formation of PK resistant PrP. PLoS Pathog. 2010; 6:e1000977. [PubMed: 20625387]

Centonze D, Muzio L, Rossi S, Furlan R, Bernardi G, Martino G. The link between inflammation, synaptic transmission and neurodegeneration in multiple sclerosis. Cell Death Differ. 2009

Choi HS, Choi YG, Shin HY, Oh JM, Park JH, Kim JI, Carp RI, Choi EK, Kim YS. Dysfunction of mitochondrial dynamics in the brains of scrapie-infected mice. Biochem Biophys Res Commun. 2014; 448:157–162. [PubMed: 24755077]

Dumont M, Kipiani K, Yu F, Wille E, Katz M, Calingasan NY, Gouras GK, Lin MT, Beal MF. Coenzyme Q10 Decreases Amyloid Pathology and Improves Behavior in a Transgenic Mouse Model of Alzheimer's Disease. J Alzheimers Dis. 2011

Eismann T, Huber N, Shin T, Kuboki S, Galloway E, Wyder M, Edwards MJ, Greis KD, Shertzer HG, Fisher AB, Lentsch AB. Peroxiredoxin-6 protects against mitochondrial dysfunction and liver injury during ischemia-reperfusion in mice. Am J Physiol Gastrointest Liver Physiol. 2009; 296:G266–274. [PubMed: 19033532]

Facecchia K, Fochesato LA, Ray SD, Stohs SJ, Pandey S. Oxidative toxicity in neurodegenerative diseases: role of mitochondrial dysfunction and therapeutic strategies. J Toxicol. 2011; 2011:683728. [PubMed: 21785590]

Fatma N, Kubo E, Sen M, Agarwal N, Thoreson WB, Camras CB, Singh DP. Peroxiredoxin 6 delivery attenuates TNF-alpha-and glutamate-induced retinal ganglion cell death by limiting ROS levels and maintaining Ca(2+) homeostasis. Brain Res. 2008; 1233:63–78. [PubMed: 18694738]

Fatma N, Kubo E, Toris CB, Stamer WD, Camras CB, Singh DP. PRDX6 attenuates oxidative stress-and TGFbeta-induced abnormalities of human trabecular meshwork cells. Free Radic Res. 2009; 43:783–795. [PubMed: 19572226]

Fatma N, Singh DP, Shinohara T, Chylack LT Jr. Transcriptional regulation of the antioxidant protein 2 gene, a thiol-specific antioxidant, by lens epithelium-derived growth factor to protect cells from oxidative stress. J Biol Chem. 2001; 276:48899–48907. [PubMed: 11677226]

Fisher AB. Peroxiredoxin 6: a bifunctional enzyme with glutathione peroxidase and phospholipase A activities. Antioxid Redox Signal. 2011; 15:831–844. [PubMed: 20919932]

Galasko DR, Peskind E, Clark CM, Quinn JF, Ringman JM, Jicha GA, Cotman C, Cottrell B, Montine TJ, Thomas RG, Aisen P. Antioxidants for Alzheimer disease: a randomized clinical trial with cerebrospinal fluid biomarker measures. Arch Neurol. 2012; 69:836–841. [PubMed: 22431837]

Gray BC, Siskova Z, Perry VH, O'Connor V. Selective presynaptic degeneration in the synaptopathy associated with ME7-induced hippocampal pathology. Neurobiology of Disease. 2009; 35:63–74. [PubMed: 19362593]

Gray BC, Skipp P, O'Connor VM, Perry VH. Increased expression of glial fibrillary acidic protein fragments and mu-calpain activation within the hippocampus of prion-infected mice. Biochem Soc Trans. 2006; 34:51–54. [PubMed: 16417481]

Guentchev M, Voigtlander T, Haberler C, Groschup MH, Budka H. Evidence for oxidative stress in experimental prion disease. Neurobiol Dis. 2000; 7:270–273. [PubMed: 10964599]

Hager K, Kenklies M, McAfoose J, Engel J, Munch G. Alpha-lipoic acid as a new treatment option for Alzheimer's disease--a 48 months follow-up analysis. J Neural Transm Suppl. 2007:189–193. [PubMed: 17982894]

Haigh CL, McGlade AR, Lewis V, Masters CL, Lawson VA, Collins SJ. Acute exposure to prion infection induces transient oxidative stress progressing to be cumulatively deleterious with chronic propagation in vitro. Free Radic Biol Med. 2011; 51:594–608. [PubMed: 21466851]

Hara MR, Snyder SH. Cell signaling and neuronal death. Annu Rev Pharmacol Toxicol. 2007; 47:117–141. [PubMed: 16879082]

Hensley K, Carney JM, Mattson MP, Aksenova M, Harris M, Wu JF, Floyd RA, Butterfield DA. A model for beta-amyloid aggregation and neurotoxicity based on free radical generation by the peptide: relevance to Alzheimer disease. Proc Natl Acad Sci U S A. 1994; 91:3270–3274. [PubMed: 8159737]

Hildeman DA, Mitchell T, Teague TK, Henson P, Day BJ, Kappler J, Marrack PC. Reactive oxygen species regulate activation-induced T cell apoptosis. Immunity. 1999; 10:735–744. [PubMed: 10403648]

Huang X, Cuajungco MP, Atwood CS, Hartshorn MA, Tyndall JD, Hanson GR, Stokes KC, Leopold M, Multhaup G, Goldstein LE, Scarpa RC, Saunders AJ, Lim J, Moir RD, Glabe C, Bowden EF, Masters CL, Fairlie DP, Tanzi RE, Bush AI. Cu(II) potentiation of alzheimer abeta neurotoxicity. Correlation with cell-free hydrogen peroxide production and metal reduction. J Biol Chem. 1999; 274:37111–37116. [PubMed: 10601271]

Immenschuh S, Baumgart-Vogt E. Peroxiredoxins, oxidative stress, and cell proliferation. Antioxid Redox Signal. 2005; 7:768–777. [PubMed: 15890023]

Jimenez-Huete A, Lievens PM, Vidal R, Piccardo P, Ghetti B, Tagliavini F, Frangione B, Prelli F. Endogenous proteolytic cleavage of normal and disease-associated isoforms of the human prion protein in neural and non-neural tissues. Am J Pathol. 1998; 153:1561–1572. [PubMed: 9811348]

Kadish I, Thibault O, Blalock EM, Chen KC, Gant JC, Porter NM, Landfield PW. Hippocampal and cognitive aging across the lifespan: a bioenergetic shift precedes and increased cholesterol trafficking parallels memory impairment. J Neurosci. 2009; 29:1805–1816. [PubMed: 19211887]

Kikuchi M, Hirosawa T, Yokokura M, Yagi S, Mori N, Yoshikawa E, Yoshihara Y, Sugihara G, Takebayashi K, Iwata Y, Suzuki K, Nakamura K, Ueki T, Minabe Y, Ouchi Y. Effects of brain amyloid deposition and reduced glucose metabolism on the default mode of brain function in normal aging. J Neurosci. 2011; 31:11193–11199. [PubMed: 21813680]

Kim IK, Lee KJ, Rhee S, Seo SB, Pak JH. Protective effects of Peroxiredoxin 6 overexpression on amyloid beta-induced apoptosis in PC12 cells. Free Radic Res. 2013

Kubo E, Fatma N, Akagi Y, Beier DR, Singh SP, Singh DP. TAT-mediated PRDX6 protein transduction protects against eye lens epithelial cell death and delays lens opacity. Am J Physiol Cell Physiol. 2008; 294:C842–855. [PubMed: 18184874]

Kubo E, Singh DP, Fatma N, Akagi Y. TAT-mediated peroxiredoxin 5 and 6 protein transduction protects against high-glucose-induced cytotoxicity in retinal pericytes. Life Sci. 2009; 84:857–864. [PubMed: 19351539]

Kuszczyk MA, Sanchez S, Pankiewicz J, Kim J, Duszczyk M, Guridi M, Asuni AA, Sullivan PM, Holtzman DM, Sadowski MJ. Blocking the interaction between apolipoprotein E and Abeta reduces intraneuronal accumulation of Abeta and inhibits synaptic degeneration. Am J Pathol. 2013; 182:1750–1768. [PubMed: 23499462]

Lafon-Cazal M, Adjali O, Galeotti N, Poncet J, Jouin P, Homburger V, Bockaert J, Marin P. Proteomic analysis of astrocytic secretion in the mouse. Comparison with the cerebrospinal fluid proteome. J Biol Chem. 2003; 278:24438–24448. [PubMed: 12709418]

Lazarini F, Boussin F, Deslys JP, Tardy M, Dormont D. Astrocyte gene expression in experimental mouse scrapie. J Comp Pathol. 1994; 111:87–98. [PubMed: 7962730]

Le Roux PD, Reh TA. Reactive astroglia support primary dendritic but not axonal outgrowth from mouse cortical neurons in vitro. Exp Neurol. 1996; 137:49–65. [PubMed: 8566212]

Lein ES, Hawrylycz MJ, Ao N, Ayres M, Bensinger A, Bernard A, Boe AF, Boguski MS, Brockway KS, Byrnes EJ, Chen L, Chen L, Chen TM, Chin MC, Chong J, Crook BE, Czaplinska A, Dang CN, Datta S, Dee NR, Desaki AL, Desta T, Diep E, Dolbeare TA, Donelan MJ, Dong HW, Dougherty JG, Duncan BJ, Ebbert AJ, Eichele G, Estin LK, Faber C, Facer BA, Fields R, Fischer SR, Fliss TP, Frensley C, Gates SN, Glattfelder KJ, Halverson KR, Hart MR, Hohmann JG, Howell MP, Jeung DP, Johnson RA, Karr PT, Kawal R, Kidney JM, Knapik RH, Kuan CL, Lake JH, Laramee AR, Larsen KD, Lau C, Lemon TA, Liang AJ, Liu Y, Luong LT, Michaels J, Morgan JJ, Morgan RJ, Mortrud MT, Mosqueda NF, Ng LL, Ng R, Orta GJ, Overly CC, Pak TH, Parry SE, Pathak SD, Pearson OC, Puchalski RB, Riley ZL, Rockett HR, Rowland SA, Royall JJ, Ruiz MJ, Sarno NR, Schaffnit K, Shapovalova NV, Sivisay T, Slaughterbeck CR, Smith SC, Smith KA, Smith BI, Sodt AJ, Stewart NN, Stumpf KR, Sunkin SM, Sutram M, Tam A, Teemer CD, Thaller C, Thompson CL, Varnam LR, Visel A, Whitlock RM, Wohnoutka PE, Wolkey CK, Wong VY, Wood M, Yaylaoglu MB, Young RC, Youngstrom BL, Yuan XF, Zhang B, Zwingman TA, Jones AR. Genome-wide atlas of gene expression in the adult mouse brain. Nature. 2007; 445:168–176. [PubMed: 17151600]

Livak KJ, Schmittgen TD. Analysis of relative gene expression data using real-time quantitative PCR and the 2(-Delta Delta C(T)) Method. Methods. 2001; 25:402–408. [PubMed: 11846609]

Malhotra JD, Kaufman RJ. ER stress and its functional link to mitochondria: role in cell survival and death. Cold Spring Harb Perspect Biol. 2011; 3:a004424. [PubMed: 21813400]

Malhotra JD, Miao H, Zhang K, Wolfson A, Pennathur S, Pipe SW, Kaufman RJ. Antioxidants reduce endoplasmic reticulum stress and improve protein secretion. Proc Natl Acad Sci U S A. 2008; 105:18525–18530. [PubMed: 19011102]

Manevich Y, Sweitzer T, Pak JH, Feinstein SI, Muzykantov V, Fisher AB. 1-Cys peroxiredoxin overexpression protects cells against phospholipid peroxidation-mediated membrane damage. Proc Natl Acad Sci U S A. 2002; 99:11599–11604. [PubMed: 12193653]

Mao P, Reddy PH. Aging and amyloid beta-induced oxidative DNA damage and mitochondrial dysfunction in Alzheimer's disease: Implications for early intervention and therapeutics. Biochim Biophys Acta. 2011; 1812:1359–1370. [PubMed: 21871956]

Markesbery WR. The role of oxidative stress in Alzheimer disease. Arch Neurol. 1999; 56:1449–1452. [PubMed: 10593298]

Mast JD, Tomalty KM, Vogel H, Clandinin TR. Reactive oxygen species act remotely to cause synapse loss in a Drosophila model of developmental mitochondrial encephalopathy. Development. 2008; 135:2669–2679. [PubMed: 18599508]

Pak JH, Choi WH, Lee HM, Joo WD, Kim JH, Kim YT, Kim YM, Nam JH. Peroxiredoxin 6 Overexpression Attenuates Cisplatin-Induced Apoptosis in Human Ovarian Cancer Cells. Cancer Investigation. 2011; 29:21–28. [PubMed: 21166495]

Pak JH, Manevich Y, Kim HS, Feinstein SI, Fisher AB. An antisense oligonucleotide to 1-cys peroxiredoxin causes lipid peroxidation and apoptosis in lung epithelial cells. J Biol Chem. 2002; 277:49927–49934. [PubMed: 12372839]

Pamplona R, Costantini D. Molecular and structural antioxidant defences against oxidative stress in animals. Am J Physiol Regul Integr Comp Physiol. 2011

Pamplona R, Naudi A, Gavin R, Pastrana MA, Sajnani G, Ilieva EV, Del Rio JA, Portero-Otin M, Ferrer I, Requena JR. Increased oxidation, glycoxidation, and lipoxidation of brain proteins in prion disease. Free Radic Biol Med. 2008; 45:1159–1166. [PubMed: 18703134]

Pankiewicz J, Asuni A, Kascak R, Kascak R, Prelli F, Vidal R, Sadowski M. Therapeutic mechanisms of anti-prion monoclonal antibodies. Alzheimer's and Dementia. 2010; 6:S555–S555.

Pankiewicz J, Prelli F, Sy MS, Kascsak RJ, Kascsak RB, Spinner DS, Carp RI, Meeker HC, Sadowski M, Wisniewski T. Clearance and prevention of prion infection in cell culture by anti-PrP antibodies. Eur J Neurosci. 2006; 23:2635–2647. [PubMed: 16817866]

Perrier V, Solassol J, Crozet C, Frobert Y, Mourton-Gilles C, Grassi J, Lehmann S. Anti-PrP antibodies block PrPSc replication in prion-infected cell cultures by accelerating PrPC degradation. J Neurochem. 2004; 89:454–463. [PubMed: 15056288]

Perry VH, Nicoll JA, Holmes C. Microglia in neurodegenerative disease. Nat Rev Neurol. 2010; 6:193–201. [PubMed: 20234358]

Peshenko IV, Novoselov VI, Evdokimov VA, Nikolaev YV, Kamzalov SS, Shuvaeva TM, Lipkin VM, Fesenko EE. Identification of a 28 kDa secretory protein from rat olfactory epithelium as a thiol-specific antioxidant. Free Radic Biol Med. 1998; 25:654–659. [PubMed: 9801064]

Phelan SA, Wang X, Wallbrandt P, Forsman-Semb K, Paigen B. Overexpression of Prdx6 reduces H2O2 but does not prevent diet-induced atherosclerosis in the aortic root. Free Radic Biol Med. 2003; 35:1110–1120. [PubMed: 14572613]

Pietri M, Caprini A, Mouillet-Richard S, Pradines E, Ermonval M, Grassi J, Kellermann O, Schneider B. Overstimulation of PrPC signaling pathways by prion peptide 106–126 causes oxidative injury of bioaminergic neuronal cells. J Biol Chem. 2006; 281:28470–28479. [PubMed: 16864581]

Raine CS. Inflammation in Alzheimer's disease: a view from the periphery. Neurobiol Aging. 2000; 21:437–440. discussion 451–433. [PubMed: 10858590]

Rhee SG, Kang SW, Jeong W, Chang TS, Yang KS, Woo HA. Intracellular messenger function of hydrogen peroxide and its regulation by peroxiredoxins. Curr Opin Cell Biol. 2005; 17:183–189. [PubMed: 15780595]

Sadowski M, Tang CY, Aguinaldo JG, Carp R, Meeker HC, Wisniewski T. In vivo micro magnetic resonance imaging signal changes in scrapie infected mice. Neuroscience Letters. 2003; 345:1–4. [PubMed: 12809974]

Sadowski MJ, Pankiewicz J, Prelli F, Scholtzova H, Spinner DS, Kascsak RB, Kascsak RJ, Wisniewski T. Anti-PrP Mab 6D11 suppresses PrP(Sc) replication in prion infected myeloid precursor line FDC-P1/22L and in the lymphoreticular system in vivo. Neurobiol Dis. 2009; 34:267–278. [PubMed: 19385058]

Saxena U. Bioenergetics breakdown in Alzheimer's disease: targets for new therapies. Int J Physiol Pathophysiol Pharmacol. 2011; 3:133–139. [PubMed: 21760971]

Schneider CA, Rasband WS, Eliceiri KW. NIH Image to ImageJ: 25 years of image analysis. Nat Meth. 2012; 9:671–675.

Shao W, Zhang SZ, Tang M, Zhang XH, Zhou Z, Yin YQ, Zhou QB, Huang YY, Liu YJ, Wawrousek E, Chen T, Li SB, Xu M, Zhou JN, Hu G, Zhou JW. Suppression of neuroinflammation by astrocytic dopamine D2 receptors via alphaB-crystallin. Nature. 2012

Siskova Z, Mahad DJ, Pudney C, Campbell G, Cadogan M, Asuni A, O'Connor V, Perry VH. Morphological and Functional Abnormalities in Mitochondria Associated with Synaptic Degeneration in Prion Disease. Am J Pathol. 2010

Spinner DS, Kascsak RB, Lafauci G, Meeker HC, Ye X, Flory MJ, Kim JI, Schuller-Levis GB, Levis WR, Wisniewski T, Carp RI, Kascsak RJ. CpG oligodeoxynucleotide-enhanced humoral immune response and production of antibodies to prion protein PrPSc in mice immunized with 139A scrapie-associated fibrils. J Leukoc Biol. 2007; 81:1374–1385. [PubMed: 17379700]

Subbarao KV, Richardson JS, Ang LC. Autopsy samples of Alzheimer's cortex show increased peroxidation in vitro. J Neurochem. 1990; 55:342–345. [PubMed: 2355227]

Tabner BJ, Turnbull S, El-Agnaf O, Allsop D. Production of reactive oxygen species from aggregating proteins implicated in Alzheimer's disease, Parkinson's disease and other neurodegenerative diseases. Curr Top Med Chem. 2001; 1:507–517. [PubMed: 11895127]

Trushina E, McMurray CT. Oxidative stress and mitochondrial dysfunction in neurodegenerative diseases. Neuroscience. 2007; 145:1233–1248. [PubMed: 17303344]

Tulsawani R, Kelly LS, Fatma N, Chhunchha B, Kubo E, Kumar A, Singh DP. Neuroprotective effect of peroxiredoxin 6 against hypoxia-induced retinal ganglion cell damage. BMC Neurosci. 2010; 11:125. [PubMed: 20923568]

Vana L, Kanaan NM, Hakala K, Weintraub ST, Binder LI. Peroxynitrite-induced nitrative and oxidative modifications alter tau filament formation. Biochemistry. 2011; 50:1203–1212. [PubMed: 21210655]

Vassallo N, Herms J. Cellular prion protein function in copper homeostasis and redox signalling at the synapse. J Neurochem. 2003; 86:538–544. [PubMed: 12859667]

Vocero-Akbani AM, Heyden NV, Lissy NA, Ratner L, Dowdy SF. Killing HIV-infected cells by transduction with an HIV protease-activated caspase-3 protein. Nat Med. 1999; 5:29–33. [PubMed: 9883836]

Wang X, Dong CF, Shi Q, Shi S, Wang GR, Lei YJ, Xu K, An R, Chen JM, Jiang HY, Tian C, Gao C, Zhao YJ, Han J, Dong XP. Cytosolic prion protein induces apoptosis in human neuronal cell SH-SY5Y via mitochondrial disruption pathway. BMB Rep. 2009; 42:444–449. [PubMed: 19643043]

Wang X, Phelan SA, Forsman-Semb K, Taylor EF, Petros C, Brown A, Lerner CP, Paigen B. Mice with targeted mutation of peroxiredoxin 6 develop normally but are susceptible to oxidative stress. J Biol Chem. 2003; 278:25179–25190. [PubMed: 12732627]

Wang Y, Phelan SA, Manevich Y, Feinstein SI, Fisher AB. Transgenic mice overexpressing peroxiredoxin 6 show increased resistance to lung injury in hyperoxia. Am J Respir Cell Mol Biol. 2006; 34:481–486. [PubMed: 16399955]

Wong BS, Brown DR, Pan T, Whiteman M, Liu T, Bu X, Li R, Gambetti P, Olesik J, Rubenstein R, Sy MS. Oxidative impairment in scrapie-infected mice is associated with brain metals perturbations and altered antioxidant activities. J Neurochem. 2001; 79:689–698. [PubMed: 11701772]

Wu YZ, Manevich Y, Baldwin JL, Dodia C, Yu K, Feinstein SI, Fisher AB. Interaction of surfactant protein A with peroxiredoxin 6 regulates phospholipase A2 activity. J Biol Chem. 2006; 281:7515–7525. [PubMed: 16330552]

Yang JW, Rodrigo R, Felipo V, Lubec G. Proteome analysis of primary neurons and astrocytes from rat cerebellum. J Proteome Res. 2005; 4:768–788. [PubMed: 15952724]

Yata K, Oikawa S, Sasaki R, Shindo A, Yang R, Murata M, Kanamaru K, Tomimoto H. Astrocytic neuroprotection through induction of cytoprotective molecules; a proteomic analysis of mutant P301S tau-transgenic mouse. Brain Res. 2011; 1410:12–23. [PubMed: 21803337]

Lay Summary

Alzheimer's and prion diseases are characterized by accumulation and deposition of misfolded proteins. In prion disease parallel with loss of subsets of nerve cells is an increase in non-neuronal cells (astrocytes) that can impact on their homeostasis. These astrocytes produce peroxiredoxin-6 (Prdx6), a protective antioxidant protein constituent of specific pathways that are activated in response to the misfolding insult and could be highly beneficial to both neuronal and non-neuronal cells. We proposed a redox regulator role for Prdx6 in regulating and maintaining normal cell function via its ability to control the cell stressors, which would contribute to amelioration of prion pathology. To confirm this we generated diseased animals with and without Prdx6 protein. Upon onset of pathology we tested the animals behaviourally, and showed that there was improvement of behavioural deficit and rescue of survival in animals with Prdx6 (Prdx6 Tg) compared to animals without Prdx6 (Prdx6 KO). Neuropathology was attenuated in the brains of Prdx6KO animals compared to Prdx6 Tg animals with disease. Furthermore application of exogenous Prdx6 rescued toxicity due to a chemical inducer of oxidative stress and a chemical inducer of cellular hypoxia in cell culture. We contend that augmentation of endogenous Prdx6 protein represents an attractive adjunct therapeutic approach for acute and chronic degenerative diseases.
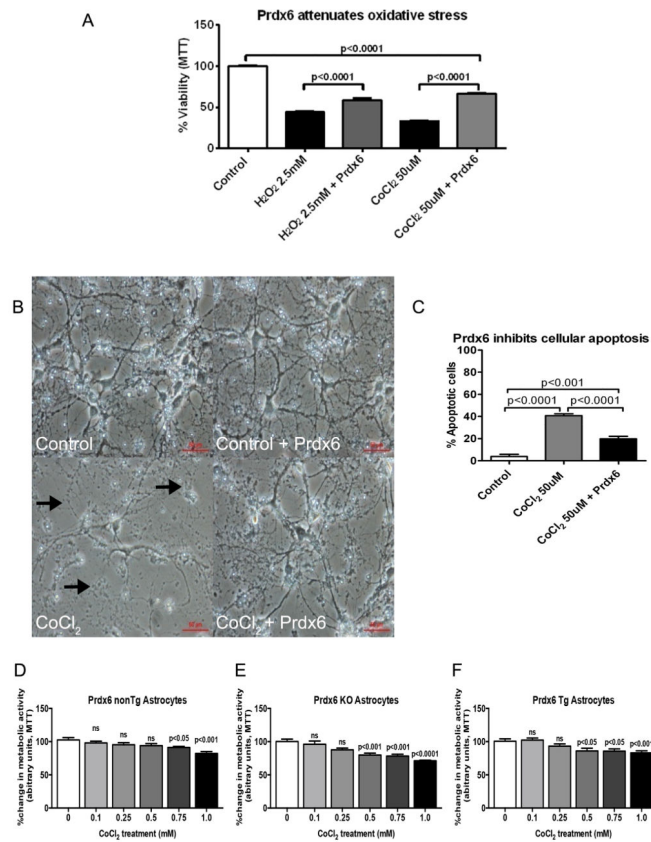
Figure 1.

(**A**) MTT assay showing that TAT-Prdx6 (5ug/ml) attenuates H_2O_2 and $CoCl_2$ mediated cytotoxicity in SK-N-SH human neuroblastoma cells. Cells were cultured and treated for 48 h with indicated concentrations of H_2O_2 and $CoCl_2$. The capacity of the cells to reduce MTT was used as a measure of cell viability, and the results are presented as the percentage of the absorbance estimated when compared with the control cells treated with DMSO only. Each bar represents a mean ± SEM. (**B** *Top panel*, and **C**): Photomicrograph of primary cortical neurons with or without $CoCl_2$ treatment, showing significant cell death in control (*left side*) compared to exogenous TAT-Prdx6 (5ug/ml) supplemented cells (*right side*). (**B** *Bottom panel*, and **C**): Cortical neurons exposed to $CoCl_2$ (*left side*) displayed significantly more evidence of apoptosis as evaluated by Hoechst stain for condensed nuclei compared to untreated control cells; in contrast to exogenous TAT-Prdx6 (5ug/ml) supplemented cells (*right side*, *p<0.0001* and *p<0.001* respectively). Arrows denote beading and dead cells. (**D, E** and **F**) There was concentration dependent increase in $CoCl_2$ toxicity in astrocytes from nonTg, Prdx6 KO and Prdx6 Tg animals. The capacity of the cells to reduce MTT was used as a measure of cell viability, and the results are presented as the percentage of the absorbance determined for control conditions (DMSO only) and represent the means ± SEM of at least three independent experiments performed in duplicate. The deleterious metabolic activity was more marked in Prdx6 KO astrocytes compared to both nonTg and Prdx6 Tg astrocytes.
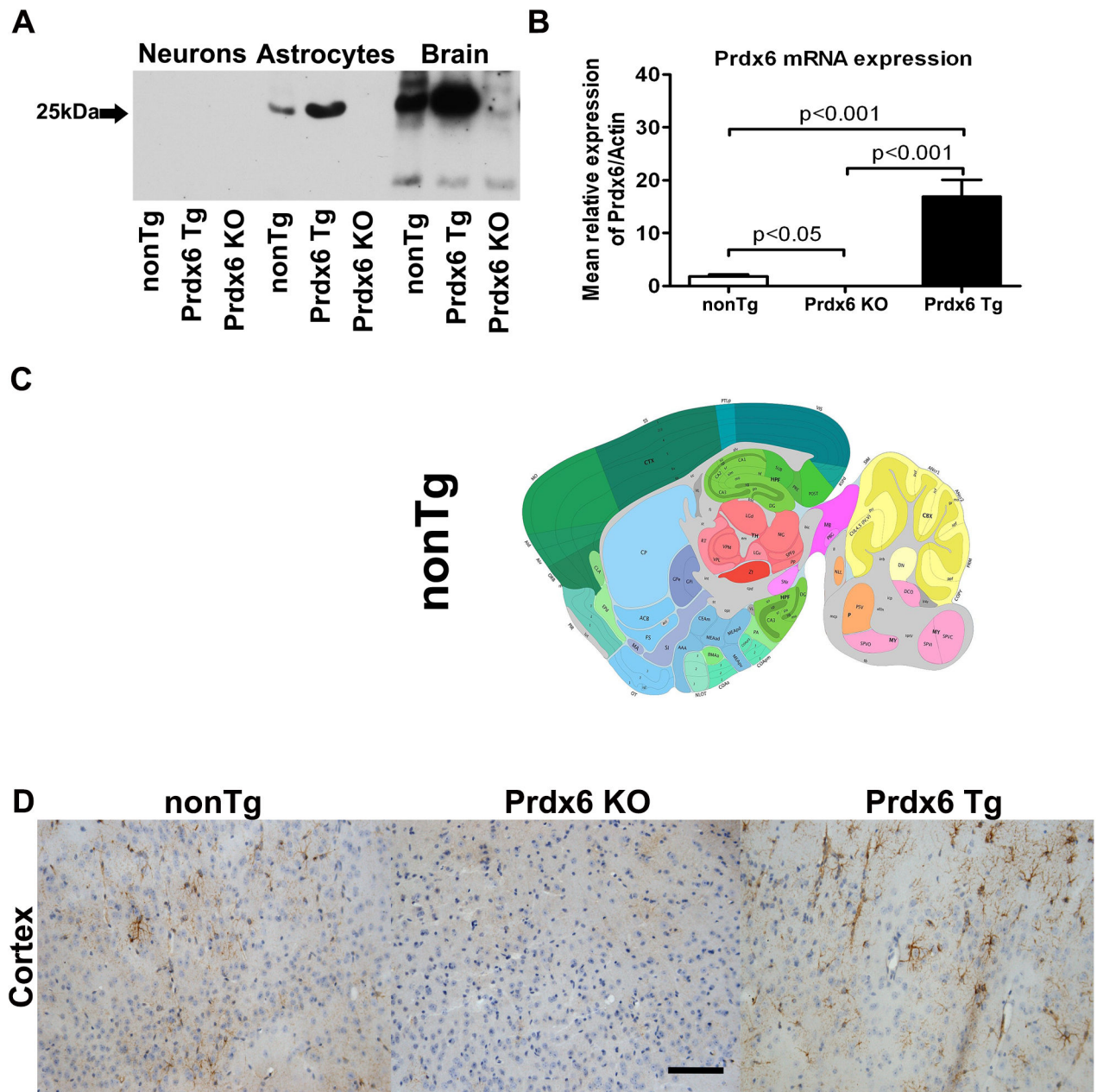
Figure 2.
Prdx6 expression in nonTg, Prdx6 Tg and Prdx6 KO animals. (**A**) Western blot analysis to confirm Prdx6 expression. Primary neurons, primary astrocytes and brain homogenates from naïve wild type nonTg, Prdx6 Tg and Prdx6 KO animals were probed for the presence of Prdx6 (Prdx6 mAb). Representative blots from 3 sets of experiments. Lane 1–3; nonTg, Prdx6 Tg, Prdx6 KO (neurons), lanes 4–6; nonTg, Prdx6 Tg, Prdx6 KO (astrocytes), lanes 7–9; nonTg, Prdx6 Tg, Prdx6 KO brain homogenates. There was no Prdx6 protein detected in either neurons, astrocytes or brain homogenates from Prdx6 KO animals, but we observed a significant 15.22-fold increase in Prdx6 protein levels in astrocytes from nonTg compared Prdx6 Tg animals (*p<0.001*) (data not shown). We observed an equally marked 4.48-fold

increase in Prdx6 protein expression in whole brain homogenates from nonTg compared Prdx6 Tg animals (*p<0.001*) (data not shown). (**B**) The brains of Prdx6 Tg mice exhibit an approximately 15-fold increase in Prdx6 mRNA compared with the nonTg animals (*p<0.001*) while there was no expression of Prdx6 mRNA in Prdx6 KO animals compared to nonTg animals (*p<0.001*). Data in graphs are presented as means ± SEM of at least three independent experiments. (**C**) Prdx6 has previously been characterized in nonTg mice by *in situ* hybridization (*upper panel*), where it is shown to be expressed in discrete regions of the brain including the cortex and hippocampus (*lower panel*). Shown in sagittal plane is the expression pattern of Prdx6 in the brain of a nonTg mouse. Probe Prdx6 - RP_040916_01_A07 - sagittal. NM_007453.2 Image credit: Allen Institute for Brain Science (Lein et al., 2007). (**D**) Immunohistological analysis of nonTg (*left panel*), and Prdx6 Tg animals (*right panel*) revealed marked Prdx6 IR but there was no Prdx6 IR in Prdx6 KO animals (*middle panel*). 20x mag, and scale bar is 100 μm.
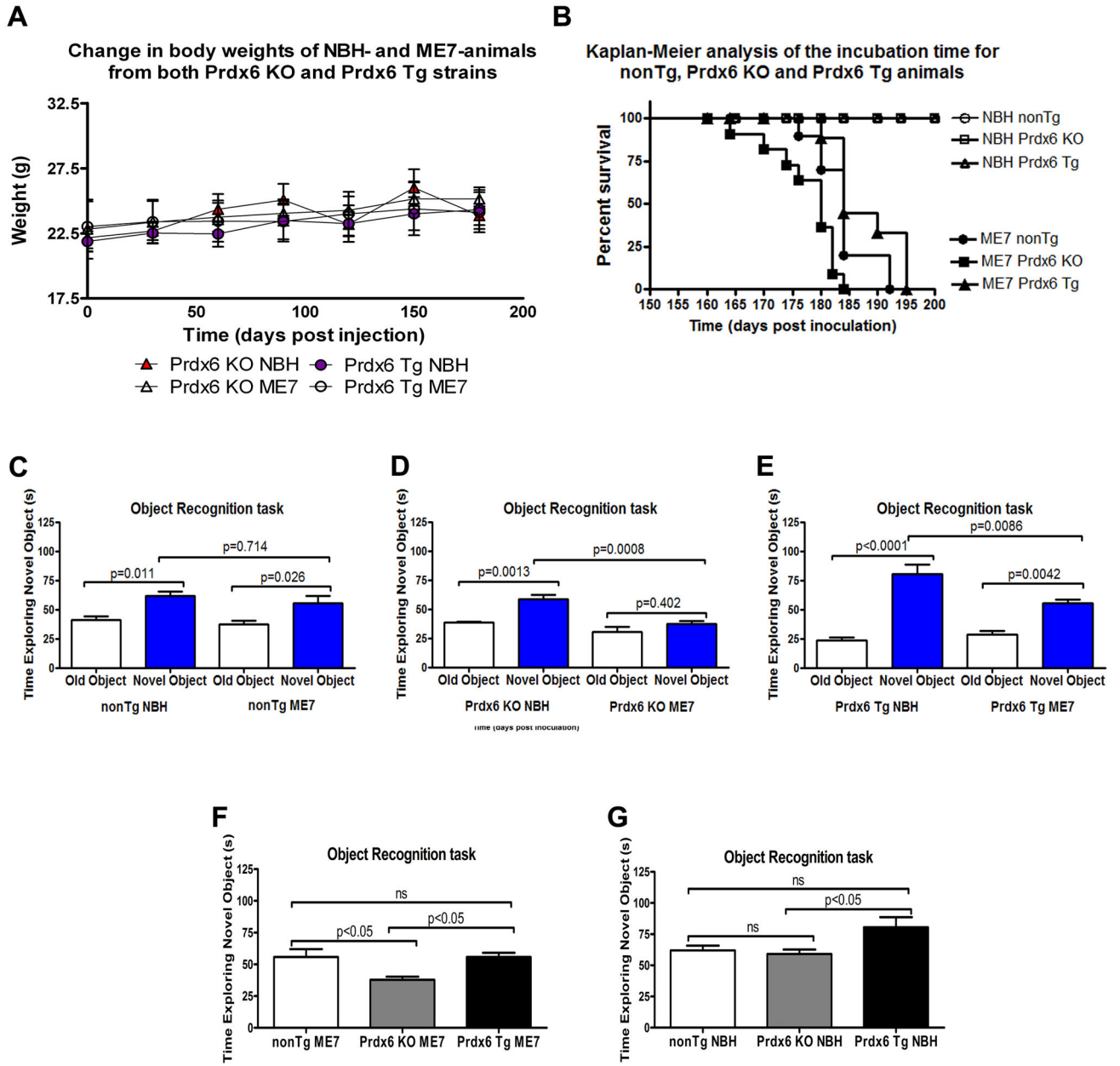
Figure 3.
(**A**) Cohorts of n = 12 were set up for the study. Animals were weighed monthly to determine if there were any atypical changes prior to eventual clinical disease onset. In the course of the study there were no significant differences in the weights of the animals. Prdx6 Tg animals weighed 22.16±0.28g, while Prdx6 KO animals weighed 21.88±0.31g respectively. (**B**) Shows prolonged survival in Prdx6 Tg animals with established prion disease. Starting at 120 dpi both NBH- and ME7-animals were tested weekly for signs of ataxia, characteristic of neuroinvasion and disease onset. Animals were sacrificed after 3 weeks of positive scoring. Differences in Kaplan-Meier survival curves of NBH and ME7 (nonTg, Prdx6 KO and Prdx6 Tg) were analyzed by the Log-rank test. All NBH and ME7

plots were significantly different (*p<0.0001*). Although nonTg ME7 compared to Prdx6 Tg ME7 was not significantly different (Mantel-Cox=2.842, df=1, *p=0.0918*, hazard ratio (HR) = 1.757), nonTg ME7 compared to Prdx6 KO ME7 was significantly different (Mantel-Cox=7.58, df=1, *p<0.0059*, hazard ratio (HR) = 0.39). Prdx6 KO ME7 compared to Prdx6 Tg ME7 was also significantly different (Mantel-Cox=12.70, df=1, *p<0.0004*, hazard ratio (HR) = 3.41). Prdx6 KO ME7 animals died within 150–185 dpi, while nonTg ME7 and Prdx6 Tg ME7 animals survived longer, living up to 192 and 195 dpi, respectively. The healthy NBH-animals were killed after 216 days. (**C**) Prior to sacrificing, mice underwent a mild cognitive test (novel object recognition task). Both nonTg ME7-animals and nonTg NBH-animals could discriminate novel from old objects (*p=0.011* and *p=0.026*, respectively) and there was no difference in their ability to discriminate novel objects (*p=0.714*). (**D**) Prdx6 KO NBH-animal could significantly discriminate novel from old objects (*p=0.0013*), whereas Prdx6 KO ME7-animals could not (*p=0.402*), and Prdx6 KO NBH-animal spent significantly more time with the novel objects than Prdx6 KO ME7-animals (*p=0.0008*). (**E**) Both Prdx6 Tg ME7-animals and Prdx6 Tg NBH-animals could discriminate novel from old objects (*p=0.0001* and *p=0.0042*, respectively) but Prdx6 Tg NBH-animals spent significantly more time with the novel object than Prdx6 ME7-animals (*p<0.0001*). (**F**) ME7 Prdx6 KO animals spent the least time with the novel objects, in contrast to nonTg ME7 and Prdx6 Tg ME7-animals (37.8% compared to 55.7%, and 55.8% for nonTg and Prdx6 Tg respectively). (**G**) Although all cohorts of NBH-animals were able to discriminate novel objects, Prdx6 Tg NBH-animals showed the most preference for the novel objects (80.56% compared to 62%, and 59% for non Tg and Prdx6 KO respectively).
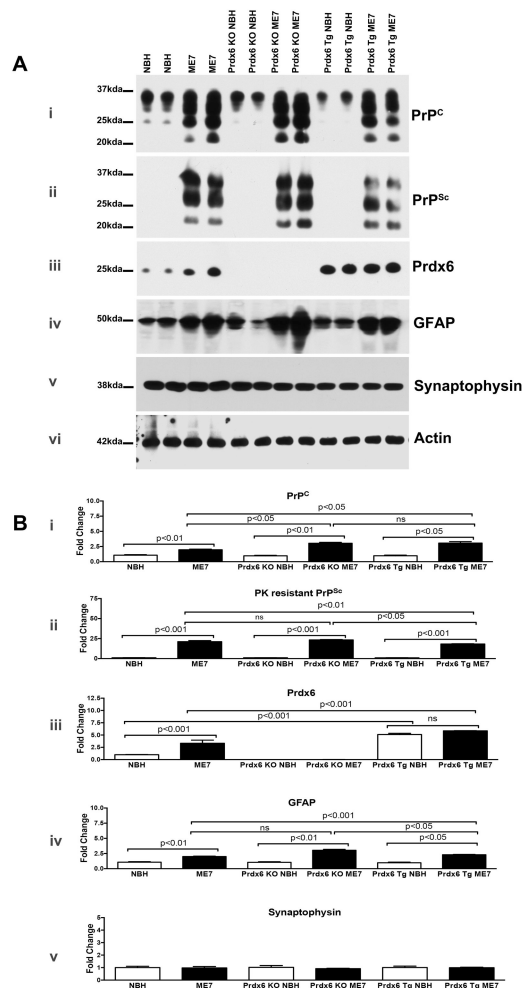
Figure 4.
Representative western blots showing change in prion related biochemistry representative of n=6 per group. We observed a significant increase in PrP immunoreactivity (IR) (PrP^C/ PrP^{Sc}) as detected by anti-PrP 6D11 mAb in nonTg, Prdx6 KO and Prdx6 Tg-ME7 compared to NBH-animals at the time point analysed (**A**; *panel i* and **B**; *graph i*). There was significantly less accumulated PK resistant PrP^{Sc} in Prdx6 Tg ME7-animals compared to Prdx6 KO-ME7-animals (**A**, *panel ii*; **B**, *graph ii; p<0.05*), but there was no significant difference in the PrP^{Sc} IR in nonTg-ME7 compared to Prdx6 KO-ME7. There was no Prdx6 expression in the cohorts of Prdx6 KO animals used (**A**, *panel iii*; **B**, *graph iii*). There was robust expression of Prdx6 protein in both Prdx6 Tg NBH- and Prdx6 Tg ME7-animals but the levels were not significantly different (**A**, *panel iii*; **B**, *graph iii;*), but the levels were significantly different from expression in nonTg animals (*p<0.001,* respectively).
GFAP IR was significantly increased in all ME7-animals, but there was significantly less in Prdx6 Tg ME7-animals compared Prdx6 KO ME7-animals (**A**, *panel iv*; **B**, *graph iv; p<0.001*).
Synaptophysin was not markedly decreased in either cohort of animals (**A**, *panel v*; **B**, *graph v)*. Statistics are based on One-way analysis of variance with Newman-Keuls Multiple Comparison Test.

non Tg ME7 hippocampus   **Prdx6 KO ME7 hippocampus**   **Prdx6 Tg ME7 hippocampus**
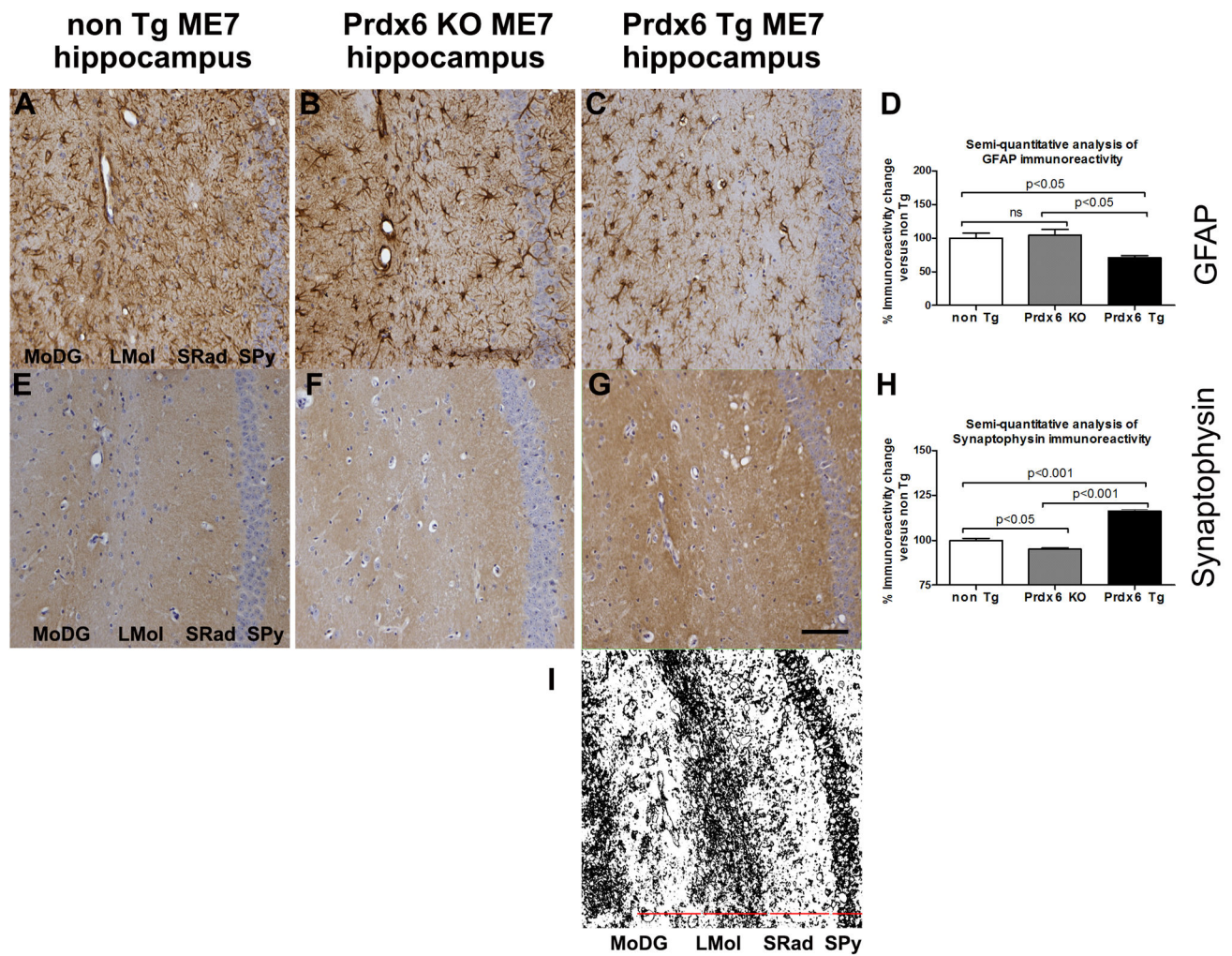
Figure 5.
Representative images of astrogliosis and synaptopathy associated with increasing accumulation of misfolded PrP^{Sc} in nonTg ME7-, Prdx6 KO ME7- and Prdx6 Tg ME7-animals. (**A–C**) anti-GFAP antibody (shows increased numbers of activated astrocytes), (**E–G**) anti-Synaptophysin antibody shows loss of demarcated synaptic layers and increasing disorganisation of synaptic architecture and decreased expression of presynaptic marker protein in nonTg ME7- and Prdx6 KO ME7-animals while a more intact synaptic architecture is revealed in Prdx6 Tg ME7-animals. These markers of prion-related pathology were all exacerbated in Prdx6 KO ME7-animals compared to Prdx6 Tg ME7-animals. No neuropathological differences were seen in Prdx6 KO NBH- and Prdx6 Tg NBH-animals (not shown here). Minus antibody control staining was also carried out (not shown). (**D**) We used ImageJ software (http://rsb.info.nih.gov/ij) to semi-quantitatively score histopathology staining and express it as a percent IR in Prdx6 KO ME7 and Prdx6 Tg ME7 relative to IR in similarly stained sections from nonTg ME7-animals (n = 3). Using this approach there was a significant decrease in GFAP IR in the hippocampus of Prdx6 Tg ME7 compared to Prdx6 KO (*p<0.001*) and nonTg ME7-animals (*p<0.001*). (**H**) Synaptophysin IR was significantly reduced in the hippocampus of nonTg ME7 (*p<0.001*) and Prdx6 KO ME7

(*p<0.001*) compared to Prdx6 Tg ME7-animals, but there was also a difference in synaptophysin IR in nonTg ME7 compared to Prdx6 KO ME7-animals. 20x mag, and scale bar is 100 μm. **(I)** Serves to show the demarcation of the synaptic layers discussed in the text. DAB staining of the representative image in (G) was identified using ImageJ software, the Colour Deconvolution plugin was used to eliminate haematoxylin counterstain, and the image threshold was adjusted. Representative images are from coronal sections showing hippocampal region, stratum pyramidal (Spy), stratum radiatum (SRad), lacunosum moleculare of the CA1 (LMol), and molecular layer of the dentate gyrus (MoDG).